Icha et al., https://doi.org/10.1083/jcb.201604095

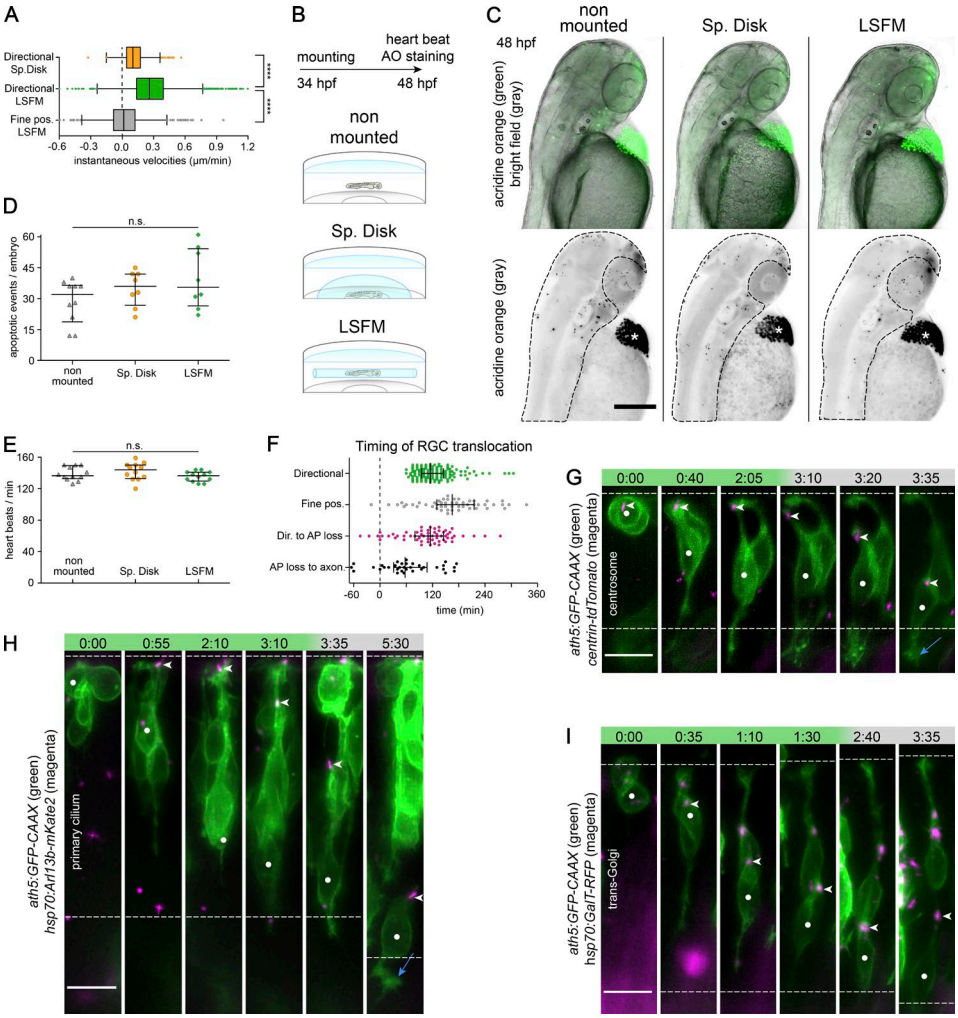

Figure S1. **Mounting is not responsible for differences between LSFM and spinning disk microscopy.** Organelle positions during RGC somal translocation. (A) Comparison of instantaneous velocities during RGC directional phase between the spinning disk confocal microscope and LSFM and between directional phase and fine positioning phases in LSFM. The values are taken from the first 95 min (or less) after mitosis or from the first 95 min of the fine positioning. The instantaneous velocities are calculated from the 1D movement along the apico–basal axis of the retina. The movement from apical to basal has a positive sign; the reverse movement has a negative sign. Directional spin disk, *n* = 21 and 4, 399 data points; directional LSFM, *n* = 140 and 24, 2,587 data points; and fine positioning LSFM, *n* = 83 and 22, 1,539 data points. 38 outliers were discarded by ROUT (Q = 1.0%) for the plotting purposes but not for the statistical testing, which was done on the whole dataset. The differences between instantaneous velocities are statistically significant: directional LSFM versus fine positioning LSFM. Mann-Whitney *U* test; ****, P < 0.0001; directional LSFM versus directional spin disk; Mann-Whitney *U* test, P < 0.0001. The data are shown as a Tukey boxplot (box shows median and interquartile range, and whiskers show 1.5 of the interquartile range). The median instantaneous velocity of directional spin disk = 0.101 µm/min, directional LSFM = 0.261 µm/min, and fine positioning LSFM = 0.015 µm/min. (B) Scheme of the experiment testing the influence of mounting for different microscopes on fish viability. The identical composition of E3 medium and agarose was used for both spin disk and LSFM mounting, and the dishes were kept together in an incubator overnight at 28.5°C. (C) Acridine orange (AO) staining for apoptotic cells. The maximum intensity projection is shown for acridine orange staining. The bright field image was created with the extended depth of field plugin in Fiji. Dashed area, area of apoptotic events count; asterisks, hatching gland. Bar, 200 µm. (D) The number of apoptotic events does not differ among the mounting strategies. *n* = 10, 8, and 8 fish, respectively. Median nonmounted = 32 events; median spin disk = 36 events; median LSFM = 36 events. Analysis of variance, P = 0.1458. (E) Heart rate does not differ among the mounting strategies. Heartbeats were counted manually for 20 s in 12 fish for each condition. Median nonmounted = 137 beats/min; median spin disk = 144 beats/min; median LSFM = 137 beats/min. Analysis of variance, P = 0.2149. (D and E) Bars represent median and interquartile range. n.s., not significant. (F) Timing of key events during RGC translocation. The duration of directional phase: median, 115 min (*n* = 140 and 24). The duration of fine positioning phase, i.e., the time from the end of directional movement to axonogenesis: median, 165 min (*n* = 50 and 19). The time from the end of directional phase to apical process (AP) loss: median, 115 min (*n* = 58 and 21). The time from apical process loss to axonogenesis: median, 57.5 min (*n* = 33 and 16). The whiskers show median and interquartile range. (G) Centrosome position during RGC translocation. *centrin-tdTomato* DNA was injected to label the centrosome together with *ath5:GFP-CAAX*. (H) Primary cilium position during RGC translocation. *hsp70:Arl13b-mKate2* DNA was injected to label primary cilium together with *ath5:GFP-CAAX*. (I) Golgi apparatus position during RGC translocation. Galactosyl transferase fragment *hsp70:GalT-RFP* DNA was injected to label trans-Golgi together with *ath5:GFP-CAAX*. (G–I) Green phase, directional movement; gray phase, fine positioning. Dashed lines delimit the apical and basal sides of the retina. White dots, RGC followed; arrowheads, organelle followed; blue arrows, axons. Time is shown in hours and minutes. Bars, 10 µm.

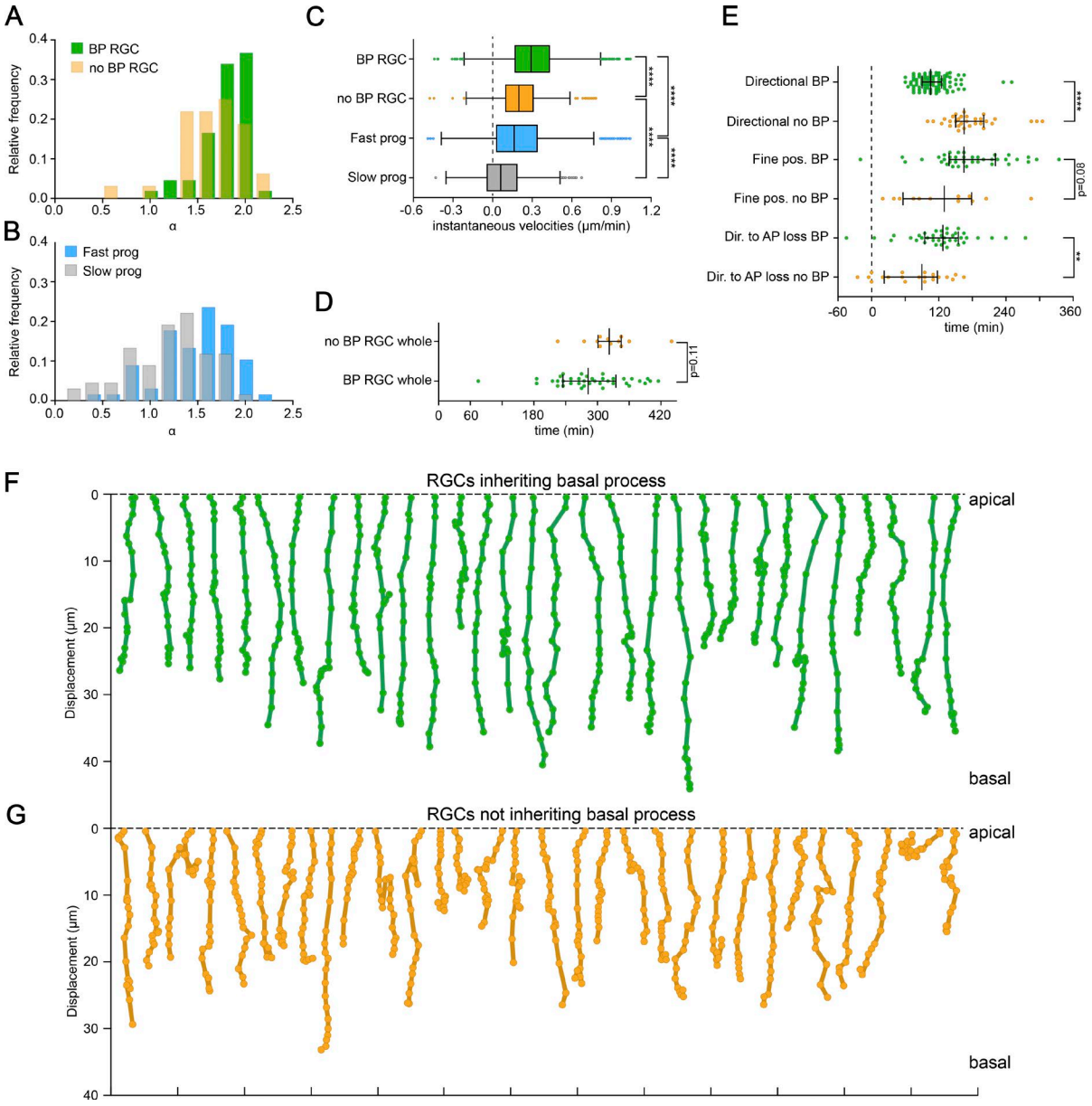

Figure S2. **Quantifications of nuclear movement in RGCs and progenitors.** (A) The α value distribution from MSDs of RGCs inheriting and not inheriting the basal process (BP) in the directional phase (data from Fig. 2 G). Median basal process RGCs = 1.83; no basal process RGCs = 1.70. The differences between α values are statistically significant: basal process RGCs versus no basal process RGCs, Mann-Whitney *U* test, P = 0.03. (B) The α value distribution from MSDs of fast and slow progenitor nuclei after mitosis (data from Fig. 2 H). Median fast progenitor = 1.53; slow progenitor = 1.26. The differences between α values are statistically significant: fast progenitors versus slow progenitors, Wilcoxon matched pairs signed rank test, P < 0.0001. (C) Comparison of instantaneous velocities among cells inheriting and not inheriting the basal process in directional phase (after mitosis). The values are taken from the first 70 min after mitosis. The instantaneous velocities are calculated from the 1D movement along the apico–basal axis of the retina. The movement from apical to basal has a positive sign; the reverse movement has a negative sign. Basal process RGC, *n* = 109 and 23, 1,526 data points; no basal process RGC, *n* = 31 and 19,448 data points; fast progenitor, *n* = 68 and 7,952 data points; slow progenitor, *n* = 68 and 7,952 data points. 45 outliers were discarded by ROUT (Q = 1.0%) for the plotting purposes, not for the statistical testing, which was done on the whole dataset. The differences between instantaneous velocities are statistically significant: basal process RGCs versus no basal process RGCs, Mann-Whitney *U* test, P < 0.0001; fast progenitors versus slow progenitors, Wilcoxon matched pairs signed rank test, P < 0.0001; no basal process RGCs versus slow progenitors, Mann-Whitney *U* test, P < 0.0001; basal process RGCs versus fast progenitors, Mann-Whitney *U* test, P < 0.0001. The data are shown as a Tukey boxplot (box shows median and interquartile ranges, and whiskers show 1.5 of the interquartile range). The median basal process RGCs = 0.29 µm/min, no BP RGCs = 0.20 µm/min, fast progenitors = 0.16 µm/min, slow progenitors = 0.06 µm/min. (D) Timing of the whole RGC translocation event (from mitosis to axonogenesis) in RGCs with and without basal process. Basal process median = 282.5 min (*n* = 38 and 18); no basal process median = 322.5 min (*n* = 12and 9); Mann-Whitney *U* test, P = 0.11. (E) Timing of events during RGC translocation depending on the basal process inheritance. Median values: directional basal process = 105 min (*n* = 109 and 23); directional no basal process = 165 min (*n* = 31 and 19); Mann-Whitney *U* test, **, P < 0.01; ****, P < 0.0001. Median values: fine positioning basal process = 165 min (*n* = 38 and 18), fine positioning no basal process = 130 min (*n* = 12 and 9); Mann-Whitney *U* test, P = 0.08. Median values: from end of directional phase to apical process loss, basal process = 127.5 min (*n* = 38 and 16); no basal process = 90 min (*n* = 20 and 15); Mann-Whitney *U* test, P = 0.003. (D and E) The median and interquartile ranges are shown. (F and G) Trajectories of RGCs inheriting (F) and not inheriting (G) the basal process. The representative 2D trajectories of 31 RGCs inheriting the basal process (F) or not (G) were plotted as manually tracked over the first 95 min after the terminal division.

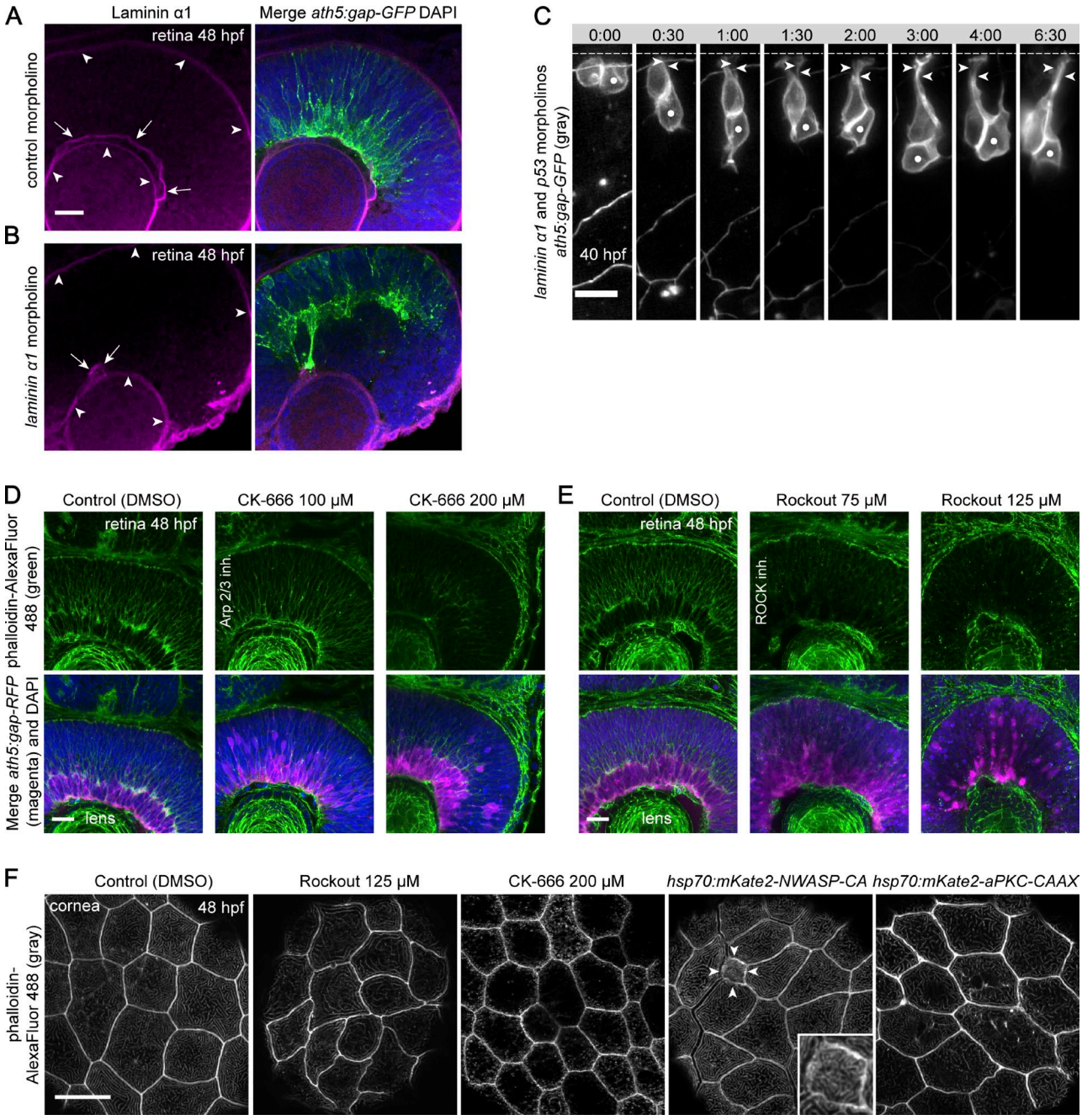

Figure S3. **RGC translocation is influenced by Laminin knockdown.** Control experiments for actin perturbations. (A) Laminin α1 distribution in control retina at 48 hpf. The Laminin channel was denoised in Fiji (ROF denoise). Note the three distinct layers of Laminin (magenta) in the developing eye and the RGCs (green) forming a basal layer of the retina. Bar, 20 μm. (B) Laminin α1 distribution after Laminin knockdown. Note that Laminin is still present in the lens and basal membrane of the retinal pigment epithelium, but is mostly absent in the retinal basal membrane, causing a tissue-wide lamination problem with the RGC layer forming in the central retina. Note that axons of RGCs associate with a small patch of Laminin left in the retinal basal membrane. (A and B) Arrows, Laminin in retina basal membrane; arrowheads, Laminin in lens and basal membrane of the retinal pigment epithelium. (C) RGC translocation is perturbed after Laminin α1 knockdown. Note that after division, the cells lose the basal process and do not translocate basally. Dashed lines delimit the apical side of the retina. White dots, RGC followed; arrowheads, apical process. Time is shown in hours and minutes. Bar, 10 μm. (D) Effect of Arp2/3 inhibition on actin cytoskeleton in the retina. Note the decreased actin staining in the 200-μM condition in the basal and central retina. The apical actin belt associated with adherens junctions is less affected. The RGC layer labeled by *ath5:gap-RFP* is disorganized. (E) Effect of ROCK inhibition on actin cytoskeleton in the retina. Note the decreased actin staining in the 75-μM and 125-μM conditions in the basal and central retina. The apical actin belt associated with adherens junctions is less affected. The RGC layer labeled by *ath5:gap-RFP* is disorganized. (F) Staining of apical actin by phalloidin in corneal cells at 48 hpf. Actin is present as two structures: it is associated with adherens junctions around the cell membranes and in microridges all over the apical membrane. The embryos were incubated with the inhibitors from 34 hpf (or heat shocked at 32 hpf) and analyzed at 48 hpf. (D–F) Bars, 20 μm. Rockout: Note that even at high Rockout concentration, the microridges persist. The cell shape, on the other hand, is more irregular compared with the control. CK-666: note the complete absence of microridges and reduced apical area of cells. NWASP-CA overexpression: this construct was injected mosaically, and the affected cell is marked with arrowheads and is shown in the inset. Note the massively reduced apical area and altered structure of microridges. aPKC-CAAX overexpression: note the altered shape of microridges and high accumulation of actin associated with adherens junctions compared with the control.

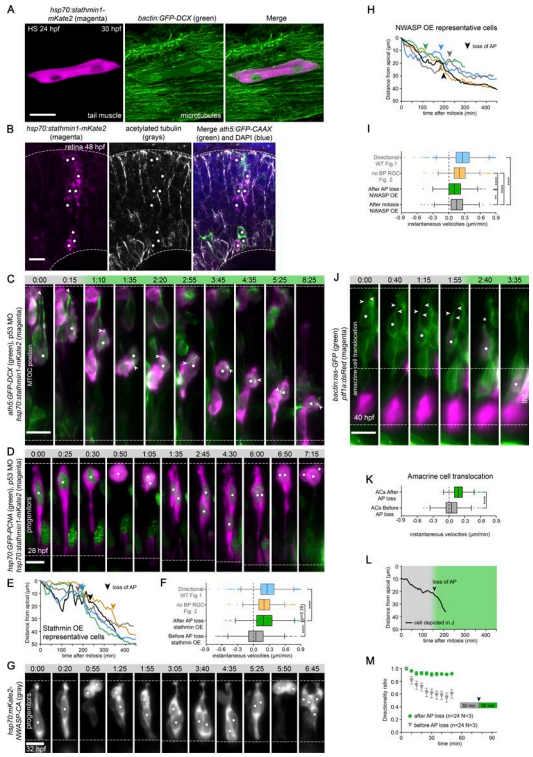

Figure S4. **Free migration of RGCs after MT destabilization or Arp2/3 inhibition and free migration of ACs.** (A) The destabilizing effect of the *hsp70:Stathmin1-mKate2* construct on MTs. The embryos of transgenic line ubiquitously expressing GFP-tagged doublecortin to label MTs were injected with *hsp70:Stathmin1-mKate2*. The fish were heat shocked (HS) around 24 hpf and imaged live 6 h later. Note the diffuse GFP-DCX signal and absence of MT filaments in the affected cell. Bar, 20 µm. (B) Stathmin overexpression decreases MT acetylation. White dots, Stathmin-overexpressing cells. Bar, 10 µm. (C) Random MT-organizing center (MTOC) position during RGC multipolar migration. MTs and MT-organizing centers were labeled by *ath5:GFP-DCX* injection. The RGC (white dots) initially has an apical MTOC (white arrowheads). The loss of apical process attachment triggers the multipolar migratory mode (time 1:10), and later the MTOC is found at a random position in the cell. Gray phase, cell still has the apical process; green phase, directional multipolar mode. The dashed lines delimit the apical and basal sides of the retina. (D) MT depolymerization by *hsp70:Stathmin1-mKate2* has no effect on the retinal progenitor cell cycle or nuclear migration. The *ath5:gap-GFP* transgenic fish were injected with the *hsp70:Stathmin1-mKate2* and *hsp70:GFP-PCNA* DNA to label nuclei. At 7:15, the *ath5:gap-GFP* expression starts. (E) Five representative trajectories of the free migrating RGCs in the Stathmin overexpression (OE) condition. 0 indicates the mitotic position of cells. The arrowheads mark the time points when the cell loses the apical process. (F) Comparison of instantaneous velocities in Stathmin overexpression before and during the multipolar migration and with control conditions. The instantaneous velocities are calculated from the 1D movement along the apico–basal axis of the retina. The movement from apical to basal has a positive sign; the reverse movement has a negative sign. Directional wild type (WT; Fig. 1), *n* = 140 and 24,2587 data points; no basal process (BP) RGC (Fig. 2), *n* = 31 and 19,448 data points; after apical process (AP) loss Stathmin overexpression (OE), *n* = 32 and 5,631 data points; before apical process loss Stathmin overexpression, *n* = 32 and 5,919 data points. Statistical significance of the differences between instantaneous velocities: directional wild type (Fig. 1) versus after apical process loss Stathmin overexpression, Mann-Whitney *U* test, P < 0.0001; after apical process loss Stathmin overexpression versus before apical process loss Stathmin, Wilcoxon matched pairs signed rank test, P < 0.0001; no basal process RGC (Fig. 2) versus after apical process loss Stathmin overexpression, Mann-Whitney *U* test, P < 0.3956. The median directional wild type (Fig. 1) = 0.26 µm/min; no basal process RGCs (Fig. 2) = 0.20 µm/min; after apical process loss Stathmin = 0.18 µm/min; before apical process loss Stathmin = 0.05 µm/min. (G) Arp2/3 inhibition by NWASP-CA has no effect on the retinal progenitor cell cycle or nuclear migration. Wild-type fish were injected with *hsp70:mKate2-NWASP-CA* and *ath5:GFP-CAAX* (not expressed in these cells) DNA. (H) Five representative trajectories of the free migrating RGCs in the NWASP-CA overexpression condition. 0 indicates the mitotic position of cells. The arrowheads mark the time points when the cell loses its apical process. (I) Comparison of instantaneous velocities in NWASP-CA overexpression before and during the multipolar migration and with control conditions. The instantaneous velocities are calculated from the trajectories of cells 95 min after mitosis and 95 after apical process loss. After apical process loss NWASP overexpression, *n* = 18 and 4,342 data points; after mitosis NWASP overexpression, *n* = 18 and 4,342 data points. Statistical significance of the differences between instantaneous velocities: directional wild type (Fig. 1) versus after mitosis NWASP overexpression, Mann-Whitney *U* test, P < 0.0001; after apical process loss NWASP overexpression versus after mitosis NWA SP overexpression, Mann-Whitney *U* test, P = 0.0013; no basal process RGC (Fig. 2) versus after apical process loss NWASP overexpression, Mann-Whitney *U* test, P < 0.0001; no basal process RGC (Fig. 2) versus after mitosis NWASP overexpression, Mann-Whitney *U* test, P < 0.0001. The median after apical process loss NWASP overexpression = 0.10 µm/min; after mitosis NWASP overexpression = 0.15 µm/min. (F and I) Outliers were discarded by ROUT (Q = 1.0%) for the plotting purposes but not for the statistical testing, which was done on the whole dataset. **, P < 0.01. (J) AC translocation. *bactin:ras-GFP*, *ptf1a:dsRed* double transgenic embryos were used as donors for blastomere transplantation into wild-type acceptors. The translocating AC (white dots) initially has the apical process (white arrowheads). Once it is lost (asterisk), fast directional movement to its final position is triggered. Gray phase, still with apical process; green phase, directional multipolar mode. The dashed lines delimit the apical side of the retina and the inner nuclear layer, where the ACs reside. (D, E, G, and J) Time is shown in hours and minutes. Bars, 10 µm. (K) Comparison of instantaneous velocities in ACs before and after apical process loss. Four outliers were discarded by ROUT (Q = 1.0%). ACs after apical process loss, *n* = 24 and 3,257 data points; ACs before apical process loss, *n* = 24 and 3,462 data points). The differences between instantaneous velocities are statistically significant: ACs after apical process loss versus ACs before apical process loss, Mann-Whitney *U* test, ****, P < 0.0001. The median ACs after apical process loss = 0.18 µm/min; ACs before apical process loss = 0.05 µm/min. (F, I, and K) The data are shown as a Tukey boxplot (box shows median and interquartile ranges, and whiskers show 1.5 of the interquartile range). (L) A representative trajectory of the translocating AC from J. The arrowhead marks the time point when the cell loses the apical process. (M) Directionality ratio of ACs before and after apical process loss. The mean of all tracks is shown with error bars representing the SEM. The interval of 50 min before and 50 min after AP loss was taken into account (arrowhead), because that is the mean duration of the directional movement after apical process loss in ACs. Final directionality ratio: ACs after apical process loss = 0.92 ACs; before apical process loss = 0.60 ACs.

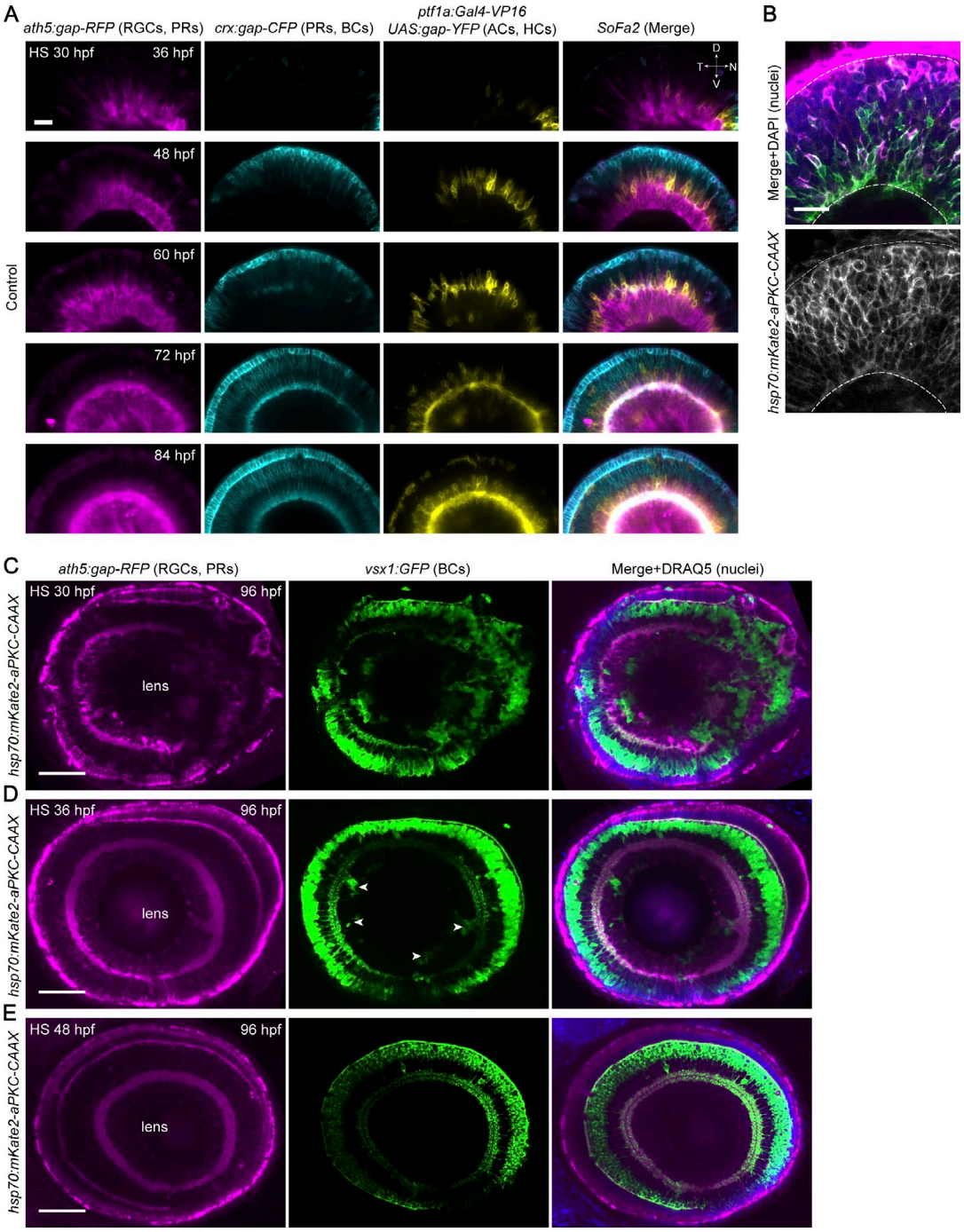

Figure S5. **The effect of aPKC-CAAX overexpression on retinal lamination and related control experiments.** (A) Control retina development. The *SoFa2* transgenic fish (combination of *ath5:gap-RFP* [labeling RGCs and photoreceptors (PRs)], *crx:gap-CFP* [labeling photoreceptors and bipolar cells (BCs)], *ptf1a:Gal4-VP16 UAS:gap-YFP* [labeling horizontal cells (HCs) and ACs]) were heat shocked (HS) at 32 hpf and imaged in the LSFM from 36 hpf every 12 h. The fish were kept in the incubator between the time points. No ectopic RGCs developed. (B) Fluorescence signal of the *hsp70:mKate2-aPKC-CAAX* construct from Fig. 6 C. Fish were heat shocked at 30 hpf, fixed at 48 hpf, and stained with Zn5 antibody. The fluorescence of mKate2-aPKC-CAAX is only detectable within 24 h of heat shock because of the fast turnover of the protein. The dashed lines mark the apical and basal membranes of the retina. (A and B) Bars, 20 µm. (C–E) aPKC-CAAX perturbs retinal lamination only during a short time window. The *ath5:gap-RFP*, *vsx1:GFP*, *hsp70:mKate2-aPKC-CAAX* triple transgenic line was heat shocked at 30 (C), 36 (D), or 48 hpf (E), fixed at 96 hpf, and stained with DRAQ5 to additionally label the nuclei. The severe lamination problems can be observed in C. Mild phenotype can be seen in D with only a few ectopic clusters of bipolar cells (arrowheads), and in E, the retina is indistinguishable from the control (Fig. 7 A) with only one continuous RGC layer and the whole retina forming an unperturbed layered structure. Bars, 50 µm.

Video 1. **Somal translocation and basal process inheritance of RGCs and progenitors.** (Part 1) Typical example of RGC translocation in LSFM, when RGC inherits the basal process. Membranes of RGCs are labeled by *ath5:gap-RFP* (gray). Time is shown in hours and minutes. Green dot, RGC during directional phase; gray dot, RGC during fine positioning phase; arrowheads, inherited basal process. (Part 2) The RGC not inheriting the basal process. Membranes of RGCs are labeled by *ath5:GFP-CAAX* (gray). Blue arrow, axon. (Part 3) Inheritance of basal process in progenitors. Membranes of cells are labeled by *bactin:mKate2 -ras* (gray), and nuclei are labeled by *hsp70:GFP-PCNA* (green). White dot, basal process inheriting progenitor; arrowheads, inherited basal process; arrows, newly formed basal process of the sister cell.

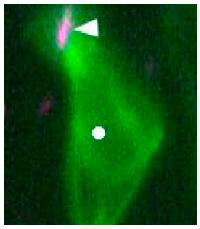

Video 2. **Organelle positions during RGC translocation.** (Part 1) Centrosome position during RGC translocation. The centrosome is labeled with *centrin-tdTomato* (magenta, white arrowhead). Membrane of RGC (white dot) is labeled by *ath5:GFP-CAAX* (green). Time is shown in hours and minutes. (Part 2) The primary cilium is labeled with *hsp70:Arl13b-mKate2* (magenta, white arrowhead). The membrane of RGC (white dot) is labeled by *ath5:GFP-CAAX* (green), and the axon is labeled by the blue arrow. (Part 3) Golgi apparatus position during RGC translocation. Golgi is labeled with *hsp70:GalT-RFP* (magenta, white arrowhead). Membrane of RGC (white dot) is labeled by *ath5:GFP-CAAX* (green).

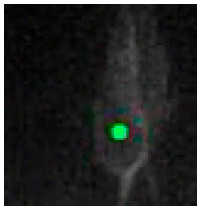

Video 3. **Live imaging of RGC translocation after ROCK inhibition.** 100 µM Rockout was added at the start of imaging. Note that RGC loses the basal process but keeps the apical process. Membranes of RGCs (green dot) are labeled by *ath5:gap-RFP* (gray). Time is shown in hours and minutes.

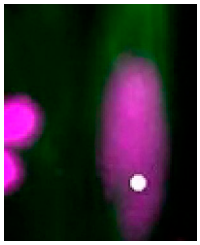

Video 4. **Live imaging of MTs in translocating RGCs.** MTs are labeled by *ath5:GFP-DCX* (green) and nuclei by *ath5 :H2B-RFP* (magenta). Note MT accumulation in the apical process. Time is shown in hours and minutes. White dot, RGC followed; blue arrow, axon.

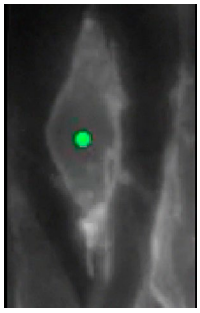

Video 5. **Multipolar migratory mode.** (Part 1) Multipolar migration in wild type. Time is shown in hours and minutes. Green dot, RGC followed. (Part 2) Multipolar migration induced by MT destabilization. Stathmin 1 (magenta) overexpression was induced at 30 hpf. Video starts at 34 hpf. Note higher protrusive activity upon loss of the basal and apical processes. White dot, RGC followed; blue arrow, axon. (Part 3) Multipolar migration induced by Arp2/3 inhibition. NWASP-CA (magenta) overexpression was induced at 30 hpf. Video starts at 34 hpf. White dot, RGC followed. (Part 4) AC translocation. *bactin:ras-GFP* (green), *ptf1a :dsRed* (magenta) double transgenic embryos were used as donors for blastomere transplantation into wild-type acceptors. The translocating AC (white dot) initially has the apical process, and its loss triggers faster directional movement to the final position.

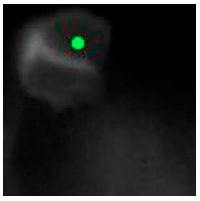

Video 6. **No RGC translocation upon aPKC-CAAX overexpression.** (Part 1) No RGC translocation upon aPKC-CAAX overexpression. Membrane of RGC is labeled by *ath5:GFP-CAAX* (gray). Time is shown in hours and minutes. Green dot, RGC followed; blue arrow, axon. (Part 2) Impaired RGC translocation upon *ath5:aPKC-CAAX* (magenta) expression. Membrane of RGC is labeled by *ath5:GFP-CAAX* (green). White dot, RGC followed; blue arrow, axon.

A script for detection of apoptotic cells is also available as a Word file.